Bachelor's Thesis

Possible Problems in Hadron Mass Calculation Using the Generalised Eigenvalue Problem

Joscha Egger

Submitted on September 29, 2022

Institute for Theoretical Physics
Max-von-Laue-Str. 1
60438 Frankfurt, Germany

Supervisor and first examiner
Prof. Dr. Marc Wagner
Institute for Theoretical Physics
Goethe University Frankfurt

Second examiner
Prof. Dr. Francesca Cuteri
Institute for Theoretical Physics
Goethe University Frankfurt

Selbstständigkeitserklärung

Erklärung nach § 30 (12) Ordnung für den Bachelor- und dem Masterstudiengang

Hiermit erkläre ich, dass ich die Arbeit selbstständig und ohne Benutzung anderer als der angegebenen Quellen und Hilfsmittel verfasst habe. Alle Stellen der Arbeit, die wörtlich oder sinngemäß aus Veröffentlichungen oder aus anderen fremden Texten entnommen wurden, sind von mir als solche kenntlich gemacht worden. Ferner erkläre ich, dass die Arbeit nicht - auch nicht auszugsweise - für eine andere Prüfung verwendet wurde.

Frankfurt, 29.09.2022

Joscha Egger

Abstract

This thesis discusses possible problems in the calculation of masses of hadrons using the generalised eigenvalue problem, or GEVP for short. In particular, an implementation of the GEVP, that has been used for years to determine masses of hadrons and has always produced reliable results, is examined for possible misbehaviour in the assignment of the obtained energies E_n. During this process, artificial data of possibly problematic systems are generated, which are then studied and analysed with the GEVP program. Subsequently, a new sorting method is implemented in the source code that corrects the issue identified in this thesis.

Contents

Chapter 1

Introduction

One of the biggest questions in physics, which Greek philosophers already addressed thousands of years ago, is the fundamental structure of the matter surrounding us. In the early 1970s, the so-called Standard Model of particle physics was developed, summarising the understanding of the structure of matter and three of the forces involved. Since then, it has successfully explained a great number of experimental results in particle physics and predicted a variety of phenomena, such as the discovery of particles. Thus, over the years, the Standard Model has established itself as a well-tested and widely known physical model.

According to the Standard Model of particle physics, all matter consists of tiny fundamental building blocks, the quarks and leptons, as well as their exchange particles, the bosons. The interaction of quarks and their exchange particles, the so-called gluons, is described by quantum chromodynamics (QCD), which plays an important role in the Standard Model. In analogy to quantum electrodynamics (QED), in which the interaction of electrically charged particles is described, QCD describes the interaction of particles with colour charge (hence the name, chromodynamics). Quarks and gluons have three different colour charges, which are arbitrarily called red, green and yellow. Altogether there are six different quarks, known as flavours, which form the hadrons and are related in three pairs, the generations. The first generation, consisting of the light up u and down d quark, makes up all the stable matter in the universe. On the other hand, the second and third generation, consisting of the charm c and strange s quark and the top t and bottom b quark, form purely unstable matter and are hundreds to several thousand times heavier than those of the first generation [1].

In recent years, numerical simulations from first principles have become a widespread and very successful technique to calculate physical observables, e.g. masses of hadrons. First principles mean that these quantities are calculated without any simplifying assumptions or approximations. This makes it possible to verify the Standard Model as the correct model of particle physics to a certain degree of accuracy, and to predict states that have not yet been experimentally discovered, like e.g. tetraquark systems. Such results can therefore provide useful hints and input for future experiments and can contribute to new physical insights [2].

Exactly such tetraquark systems are studied, for example, in our working group. To

determine hadron masses, a program based on the so-called generalised eigenvalue problem has been used for years and has since provided reliable results. However, the suspicion arose that incorrect assignments of the energy levels could occur in a small number of constellations. Since this program is used for ongoing research in our working group, the task of this thesis was to identify possible erroneous behaviour and to find and implement a solution for this.

This thesis is structured as follows: First, chapter 2 deals with the theoretical fundamentals that are essential for understanding the thesis. In particular, quantum chromodynamics generally, techniques of lattice QCD and the generalised eigenvalue problem are covered, all of which are important parts of this work. Subsequently, in chapter 3 the approach to the issue of this thesis is shown and how it was corrected by a sorting of the eigenvectors $v_n(t)$ and eigenvalues $\lambda_n(t)$. In chapter 4, results of the newly implemented code extension are presented and analysed both from artificially generated data and from real data. Finally, in chapter 5 the results are briefly summarised, conclusions are drawn and outlooks are given.

Chapter 2

Theoretical Basics

2.1 Quantum Chromodynamics

Quantum chromodynamics (QCD) is a quantum field theory that describes the strong interaction, i.e. the interaction of quarks mediated by gluons. Together they are the constituents of the hadrons, which include the mesons ($\bar{q}q$ states, such as the pion π or the kaon K) and the baryons (qqq states, such as the proton p or the neutron n).

2.2 Lattice QCD

In QCD, the interacting quarks and gluons are described by quantum fields that propagate throughout continuous space at all times. To solve the resulting equations exactly, one would have to calculate infinite-dimensional integrals, which is, however, impossible in practice. One of the best established non-perturbative approaches to solving this issue is lattice QCD. As the name implies, lattice QCD circumvents the problem by reducing the continuous spacetime to discrete spacetime points, the lattice, and thereby making the integrals finite-dimensional. To this end, several actions are taken for the following contents [2, 3]:

- The Euclidean time evolution is used (Wick rotation): $t \rightarrow -i\,t$.
- The spacetime is discretised: $x_\mu \in \mathbb{R}^4 \rightarrow x_\mu = n_\mu \times a,\ n_\mu \in \mathbb{Z}^4$, where a denotes the lattice spacing.
- A discrete energy eigenvalue spectrum is assumed, where $E_\Omega \leq E_0 \leq E_1 \ldots$.
- The spacetime is considered periodic: $x_\mu \equiv x_\mu + L\,e_\mu(\nu)$, with $L = a\,N_a$, where $e_\mu(\nu)$ denotes the unit vector in ν direction and N_a the number of lattice sites in each spacetime direction.

A commonly calculated observable in lattice QCD from which physical properties, such as energy spectra, can be obtained is the temporal correlation function or

correlation matrix, which is defined in the following way:

$$C_{jk}(t) = \left\langle \mathcal{O}^j(t)\, \mathcal{O}^{k\,\dagger}(0) \right\rangle = \frac{1}{Z} \int \mathcal{D}[\Phi]\, O^j[\Phi(.,t)]\, O^{k\,\dagger}[\Phi(.,0)]\, \mathrm{e}^{-S_E[\Phi]} \ , \tag{2.1}$$

with the normalisation factor $Z = \sum_n \mathrm{e}^{-E_n\, T}$ and the periodic temporal expansion of the lattice T. The right-hand side of the equation is the Euclidean path integral over all possible configurations of the gauge field Φ. For this purpose, the operators of the two interpolating fields $\mathcal{O}^j$ and $\mathcal{O}^k$ were translated into functionals and the Boltzmann factor was multiplied into the integral, containing the classical Euclidean action $S_E[\Phi]$. This weighting factor is used to perform an importance sampling and to evaluate the integral on the basis of it. Using stochastic integration techniques (so-called Monte Carlo algorithms) this type of integral can be calculated numerically, whereby the temporal correlation function is obtained. The middle part of the equation, i.e. the correlation function, can be expanded for further use as follows [4–7]:

$$\begin{aligned} \left\langle \mathcal{O}^j(t)\, \mathcal{O}^{k\,\dagger}(0) \right\rangle &= \frac{1}{Z} \sum_{m,n} \langle m | \mathrm{e}^{-\mathcal{H}\,(T-t)}\, \mathcal{O}^j\, \mathrm{e}^{-\mathcal{H}\,t} | n \rangle\, \langle n | \mathcal{O}^{k\,\dagger} | m \rangle \\ &= \frac{1}{Z} \sum_{m,n} \mathrm{e}^{-E_m\,(T-t)}\, \psi^j_{mn}\, \mathrm{e}^{-E_n\,t}\, (\psi^k_{mn})^* \ , \end{aligned} \tag{2.2}$$

with $\psi^j_{mn} = \langle m | \mathcal{O}^j | n \rangle$, the Hamiltonian $\mathcal{H}$ of the system, the energy eigenstates $|n\rangle$ and the corresponding energy eigenvalues E_n. When we now extract the vacuum energy factor $\mathrm{e}^{-E_\Omega\, T}$ from both the numerator and the denominator and, for convenience, use E_n to denote the energy differences relative to the vacuum henceforth (i.e. E_n instead of $E_n - E_\Omega$), we obtain:

$$\left\langle \mathcal{O}^j(t)\, \mathcal{O}^{k\,\dagger}(0) \right\rangle = \frac{\sum_{m,n} \mathrm{e}^{-E_m\,(T-t)}\, \psi^j_{mn}\, \mathrm{e}^{-E_n\,t}\, (\psi^k_{mn})^*}{1 + \mathrm{e}^{-E_0\,T} + \mathrm{e}^{-E_1\,T} + \ldots} \ . \tag{2.3}$$

Considering the limit $T \to \infty$, only the terms with $|m\rangle = |\Omega\rangle$ (i.e. $E_m = 0$) remain in the numerator and the denominator becomes equal to 1. This gives us an expression from a sum of exponentials, where each exponent corresponds to an energy level:

$$\lim_{T\,\to\,\infty} \left\langle \mathcal{O}^j(t)\, \mathcal{O}^{k\,\dagger}(0) \right\rangle = \sum_n \psi^j_n\, (\psi^k_n)^*\, \mathrm{e}^{-E_n\,t} \ , \tag{2.4}$$

with $\psi^j_n = \langle \Omega | \mathcal{O}^j | n \rangle$. For sufficiently large t, the terms with $n > 0$ are strongly suppressed, since in general $E_n > E_0 \ \forall \ n > 0$. Thus, the ground state energy E_0 can be calculated from the exponential decay of the temporal correlation function.

2.3 Generalised Eigenvalue Problem

A well-known and quite common technique for analysing correlation matrices is the so-called GEVP method. The extraction of several energy levels can thereby be achieved by solving the generalised eigenvalue problem (GEVP)

$$C(t)\, v_n(t,t_0) = \lambda_n(t,t_0)\, C(t_0)\, v_n(t,t_0), \ n = 0, \ldots, N-1, \ t > t_0 \ , \tag{2.5}$$

with the correlation matrix $C(t)$, the eigenvectors $v_n(t, t_0)$, the corresponding eigenvalues $\lambda_n(t, t_0)$ and a variable input parameter t_0. If we now use Eq. (2.4) and select appropriate states $|n\rangle$, with $n = 0, \ldots, N-1$, the entries of the resulting truncated correlation matrix

$$\widetilde{C}_{jk}(t) = \sum_{n=0}^{N-1} \psi_n^j \, (\psi_n^k)^* \, \mathrm{e}^{-E_n \, t} \tag{2.6}$$

approximate the correlation matrix $C(t)$ from Eq. (2.5) rather well, which is why we consider them equivalent in the following [8]. In order to use this equation for the GEVP method, we first introduce the dual (time independent) vectors $u_n \propto v_n(t, t_0)$ defined by $(u_n, \psi_m) = \delta_{mn}, \; m, n < N$. We then multiply these from the right to Eq. (2.6) to obtain [9, 10]:

$$\begin{aligned} C(t)\, u_n &= \mathrm{e}^{-E_n \, t} \, \psi_n \\ &= \lambda_n(t, t_0) \; \underbrace{C(t_0)\, u_n}_{= \mathrm{e}^{-E_n t_0} \, \psi_n} \; . \end{aligned} \tag{2.7}$$

Comparing the upper with the lower part of this equation, it is immediately obvious that $\lambda_n(t, t_0)$ and E_n have a simple mathematical relationship:

$$\lambda_n(t, t_0) = \mathrm{e}^{-E_n \, (t - t_0)} \; . \tag{2.8}$$

From the eigenvalues $\lambda_n(t, t_0)$, the effective energies $E_n^{\mathrm{eff}}(t, t_0)$ can subsequently be defined as follows:

$$\begin{aligned} E_n^{\mathrm{eff}}(t, t_0) &= \frac{1}{a} \, \ln \left(\frac{\lambda_n(t, t_0)}{\lambda_n(t + a, t_0)} \right) \, , \\ E_n &= \lim_{t \, \to \, \infty} E_n^{\mathrm{eff}}(t, t_0) \, , \end{aligned} \tag{2.9}$$

where the effective energies are time-dependent and form plateaus for large times t. To obtain the energies E_n from these in the next step, t is chosen as large as necessary so that the plateaus are reached, but at the same time the errors are as small as possible. Thus, by solving the GEVP of a given correlation matrix $C(t)$, one can simply obtain a number of N energies E_n, which is why the GEVP method so commonly used.

An important orthogonality of the vectors u_n, that will be used later in this work, has the following form:

$$\langle u_m | C(t)\, u_n \rangle = \delta_{mn} \, \mathrm{e}^{-E_n \, t} \tag{2.10}$$

and is valid for all times t.

Chapter 3

Approach and Implementation

3.1 The Code

The program was developed by Prof. Dr. Marc Wagner during his dissertation in order to obtain energy levels and masses of different systems of hadrons. The programming language used is C / C++ and the functionality is based on the GEVP method described in chapter 2.3.

In order to use the code and therefore the compiled program, the temporal correlation matrix matrix $C(t)$ of the system to be analysed is needed. As already mentioned in section 2.2, this can be obtained numerically, using Monte Carlo algorithms, for example. With the help of the GNU Scientific Library (GSL), the program solves the generalised eigenvalue problem (2.5) of the correlation matrix averaged over all samples and calculates the N effective energies $E_n^{\text{eff}}(t)$ with Eq. (2.9) [11]. For the error calculation, the so-called jackknife method is used. Here, the GEVP is additionally calculated for all reduced samples (where one sample was removed in each case during the averaging of the correlation matrix), with which a statistical error can be determined (see for example [12]).

3.2 Identifying the Source(s) of Error

At the beginning of the work, it was not entirely clear where an improvement of the code might be appropriate, since this implementation of the generalised eigenvalue problem has provided reliable results for analyses and computations for years. However, it was suspected that in a few rare cases the energy levels might be sorted and thus assigned incorrectly. Two problematic situations came to mind, which could possibly lead to the effective energies being mixed up:

1. Effective energy plateaus very close to each other: Energies E_n that differ only minimally could become indistinguishable with increasing t due to their errors, which could lead to incorrect assignments.

2. Intersecting effective energies $E_n^{\text{eff}}(t)$: Since the effective energies form plateaus with increasing t, a prior overlapping of these could lead to unwanted mix-ups.

In the following sections, artificial data of possibly problematic systems are generated and subsequently analysed for potential unintended behaviour of the program (e.g. incorrect assignments) in order to specifically check these assumptions.

3.2.1 Artificial Data

Since the code uses correlation matrices for calculating the effective energies, these must consequently be generated artificially. This is achieved using a self-written program that calculates the entries of the correlation matrices via Eq. (2.6) and then adds an uncorrelated Gaussian error with the standard deviation σ. To avoid introducing unnecessary complexity and possible sources of error into the system, we initially assume 2×2 correlation matrices

$$C(t) = \sum_n \begin{pmatrix} (\psi_n^1)^2 & \psi_n^1 \, \psi_n^2 \\ \psi_n^2 \, \psi_n^1 & (\psi_n^2)^2 \end{pmatrix} \mathrm{e}^{-E_n \, t} \ , \tag{3.1}$$

where the states E_n and the prefactors ψ_n^j are chosen in such a way that the problematic systems and situations described in the previous section arise.

3.2.2 Findings

Let us now examine the first problematic scenario, i.e. systems with energy levels close to each other. For this we assume the simplest case, with two decoupled states, resulting in a diagonalised correlation matrix and use comparable large errors ($\sigma \approx 10^{-4}$). Therefore, we construct the operator $\mathcal{O}^1$ with an overlap to the first state E_0 and the operator $\mathcal{O}^2$ with an overlap to the second state E_1. Figure 3.1 shows both the effective energies $a\,E_n^{\mathrm{eff}}(t)$ of two such systems and the corresponding normalised eigenvector components $|v_n^j(t)|^2$. At first glance as well as on closer inspection, no wrong behaviour can be seen. Although the effective energies are occasionally the other way round for increasing t, this is not a sign of a false result. On the one hand, the error bars (i.e. the uncertainties) are quite large here and, on the other hand, one must always consider that the effective energies are calculated via the ratio of the eigenvalues $\lambda_n(t)$ and $\lambda_n(t+a)$. Thus, different errors in t and $t+a$ can lead to such momentary swaps. The eigenvector components behave as theoretically expected as well.

	left system				right system		
n	ψ_n^1	ψ_n^2	$a\,E_n$	n	ψ_n^1	ψ_n^2	$a\,E_n$
0	1.0	0	0.59	0	1.0	0	0.54
1	0	1.0	0.61	1	0	1.0	0.56

Table 3.1: Input parameters of the artificial data shown in Figure 3.1.

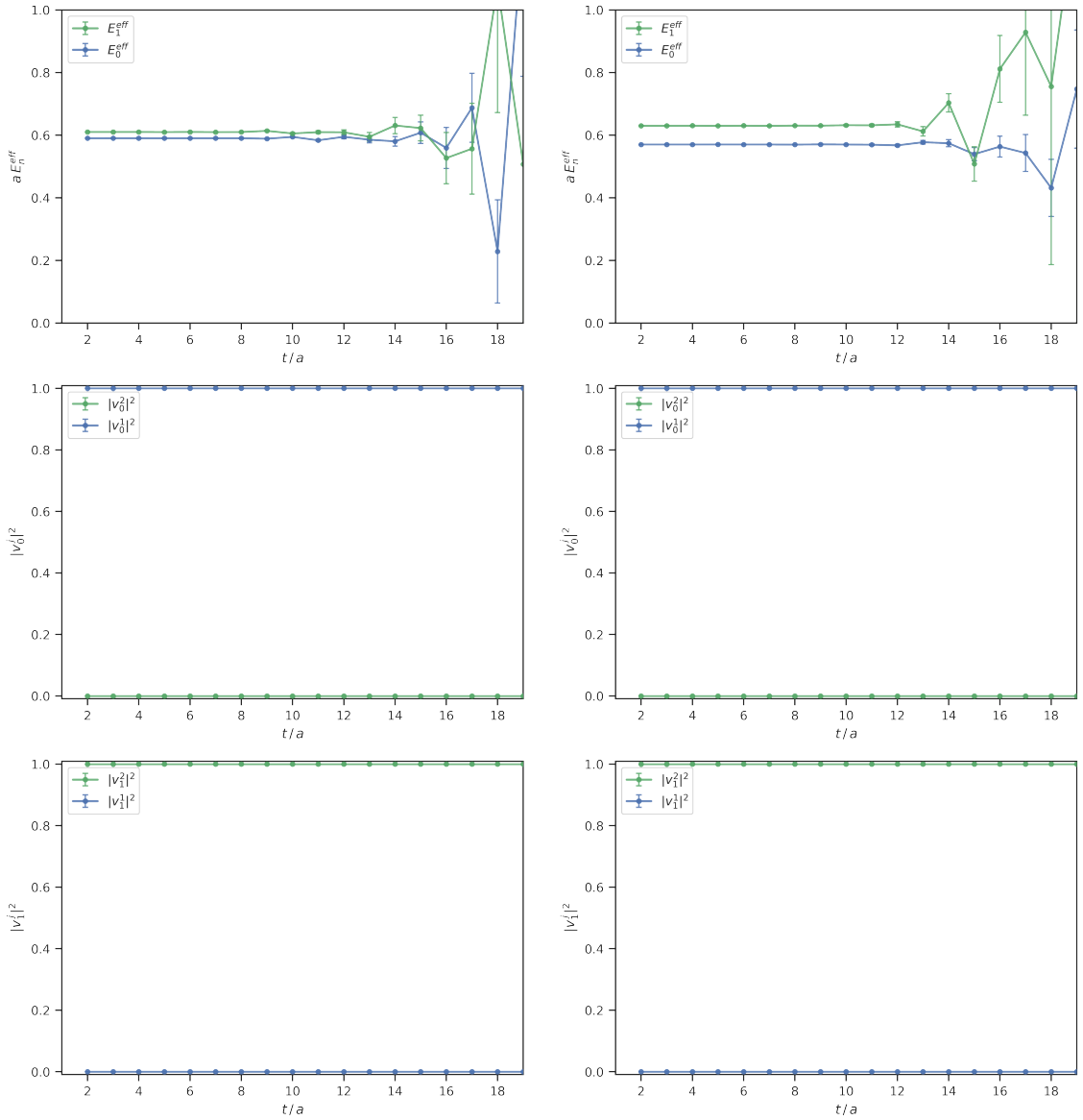

Figure 3.1: Effective energies $a\,E_n^{\text{eff}}(t)$ and normalised eigenvector components $|v_n^j(t)|^2$ of two artificial systems.

Secondly, we consider the situation where the two effective energies $E_n^{\text{eff}}(t)$ cross. Again, we assume the simplest case, with three decoupled states and use small errors ($\sigma \approx 10^{-5}$). Hence, we construct the operator $\mathcal{O}^1$ with both an overlap to the first state E_0 and the third state E_2 and the operator $\mathcal{O}^2$ with only an overlap to the second state E_1. Figure 3.2 again shows the effective energies $a\,E_n^{\text{eff}}(t)$ and the normalised eigenvector components $|v_n^j(t)|^2$ of two such systems, where one can immediately see that these results cannot be correct. In the left plot, the energies intersect as expected at $t \approx 3$, but at $t = 7$ the two curves oddly swap. The same behaviour occurs with the eigenvector components underneath. At the moment when the effective energies switch, they also switch. The rest of the plots then correspond to the expectations, except that the assignments are swapped. It is also noticeable that the effective energies do not simply swap, but that one data point is lowered or raised respectively. Thus, the energy levels bend in the direction of

the other energy level before the erroneous swap. Since the energies are calculated from the ratio of the eigenvalues $\lambda_n(t)$ and $\lambda_n(t+a)$, this misbehaviour is probably related to the sorting of the eigenvalues. It is therefore logical that we take a closer look at the eigenvalues in the following.

	left system				right system		
n	ψ_n^1	ψ_n^2	$a\,E_n$	n	ψ_n^1	ψ_n^2	$a\,E_n$
0	0.7	0	0.2	0	0.2	0	0.3
1	0	1.0	0.3	1	0	1.0	0.5
2	1.0	0	1.0	2	1.0	0	1.0

Table 3.2: Input parameters of the artificial data shown in Figure 3.2.

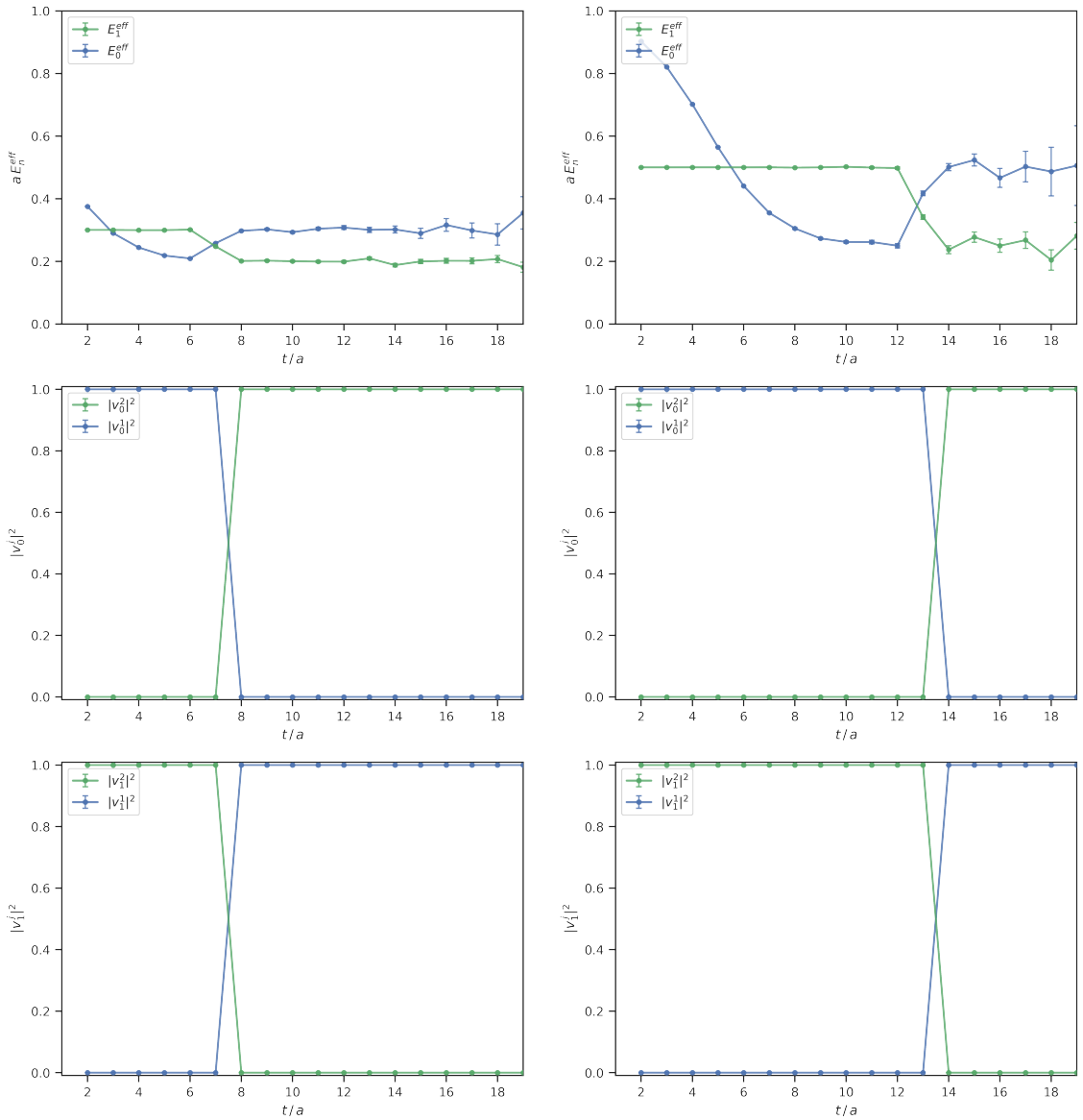

Figure 3.2: Effective energies $a\,E_n^{\text{eff}}(t)$ and normalised eigenvector components $|v_n^j(t)|^2$ of another two artificial systems.

In Figure 3.3 the eigenvalues $\lambda_n(t)$ of the left system from Figure 3.2 are plotted. At the time when the swap occurs in the effective energy plot, the eigenvalues λ_1 and λ_2 are tangent to each other and have a small kink in their curve. It is particularly noticeable that the eigenvalues do not intersect, contrary to their apparent progression. The larger eigenvalue is thereby assigned to the same effective energy $E_1^{\text{eff}}(t)$ at every time t, which seems incorrect.

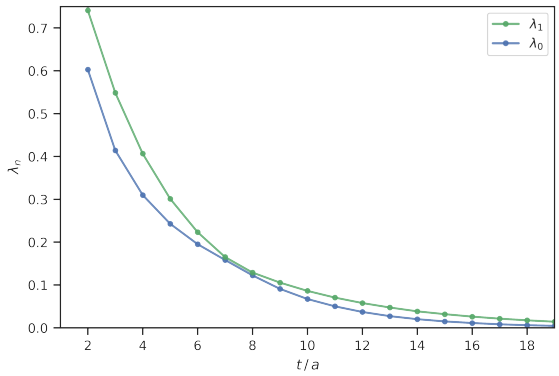

Figure 3.3: Eigenvalues $\lambda_n(t)$ of the left system in Figure 3.2.

With the source code, this undesired behaviour can be understood. The program sorts the eigenvalues in descending order so that the largest eigenvalue always belongs to the same effective energy. In many cases this matching is correct, however, as this example shows, this is not always the case. We therefore have to implement a code extension that sorts the eigenvalues in a different and logical way.

3.3 Enhancing the Code

A reasonable sorting can be achieved using Eq. (2.10). This is because the eigenvectors $v_n(t)$ obtained by the GEVP are orthogonalised in the base of the correlation matrix $C(t_0)$. Hence, it can be determined which eigenvalue $\lambda_m(t)$ and related eigenvector $v_m(t)$ belong to each effective energy $E_n^{\text{eff}}(t)$, resulting in a correct sorting.

To implement this sorting method, the scalar product of all eigenvectors in the base of the correlation matrix must first be normalised. This is achieved as follows:

$$\hat{v}_n(t) = \frac{1}{\sqrt{\langle v_n(t)|C(t_0)\, v_n(t)\rangle}}\, v_n(t) \;\rightarrow\; \langle \hat{v}_m(t)|C(t_0)\, \hat{v}_n(t)\rangle = \delta_{mn}\ . \tag{3.2}$$

The next step is to define a reference time t^{ref}, chosen at the moment when the plateaus of effective energies $E_n^{\text{eff}}(t)$ first form, and which is later set by the user. The program then calculates the scalar product $\langle \hat{v}_m(t)|C(t_0)\, \hat{v}_n(t^{\text{ref}})\rangle$ for all m and assigns the eigenvalue $\lambda_m(t)$ and associated eigenvector $v_m(t)$ for which the scalar product becomes maximal to the effective energy $E_n^{\text{eff}}(t)$ (due to the normalisation ≈ 1). This procedure is then repeated for all n and t and carried out for the sample as well as for all subsamples. The resulting sorting of the eigenvalues and eigenvectors should thus solve the problem of incorrect assignments.

3.4 Instructions for Using the Extension

The sorting function has been implemented as an extension to the persistent program so that the operation is fairly straightforward. First, one has to plot the effective energies $E_n^{\text{eff}}(t)$ as prior to the extension and then take the reference time t^{ref} from them. As already described in the section 3.3, the reference time should be chosen at the moment when the plateaus of the effective energies first form. It should be noted that data, for which no plateaus are formed and therefore no reference time can be chosen, are physically nonsensical. In order to use the extended sorting function, one only has to insert the following line into the script file under each calculation of the effective energies $E_n^{\text{eff}}(t)$ and eigenvectors $v_n(t)$:

$$\text{SORTING\_GEP } \underbrace{t^{\text{ref}}\ t^{\text{ref}}\ \ldots\ t^{\text{ref}}}_{N \text{ times}}$$

with the number of effective energies N. As a result, the updated sorting method is used in the calculations.

Chapter 4

Results

First, we re-analyse the artificial data generated in section 3.2 with the newly implemented sorting method and check whether the false results are rectified. The next step is then to apply the code extension to real data and compare these results with those of the original program.

4.1 Artificial Data

Here we first take a look at the eigenvalues $\lambda_n(t)$, which were already discussed in the previous chapter. Figure 4.1 shows the eigenvalues from Figure 3.3, except that they have now been re-sorted with the new code extension, using $t^{\text{ref}} = 9$. One can directly see the behaviour we expected, namely an intersection of the two eigenvalues between $t = 7$ and $t = 8$. The two exponentially decreasing curves therefore no longer have a discontinuous slope, suggesting that the sorting was successful.

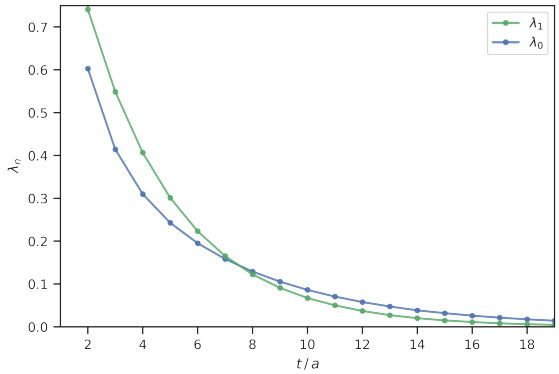

Figure 4.1: Newly sorted eigenvalues $\lambda_n(t)$ of the left system in Figure 3.2.

When looking at the effective energies $E_n^{\text{eff}}(t)$ and the normalised eigenvector components $|v_n^j(t)|^2$, shown in Figure 4.2, one can clearly see the differences and improvements to the previous results (Figure 3.2). Both the swapping of the energy levels and the eigenvector components as well as the previous bending in the direction of the respective other energy levels no longer occur. The results with the new sorting of the eigenvalues thus now agree with the theoretical expectations and no longer

show the unintended swapping. For the new sorting method, $t^{\text{ref}} = 9$ was used for both plots.

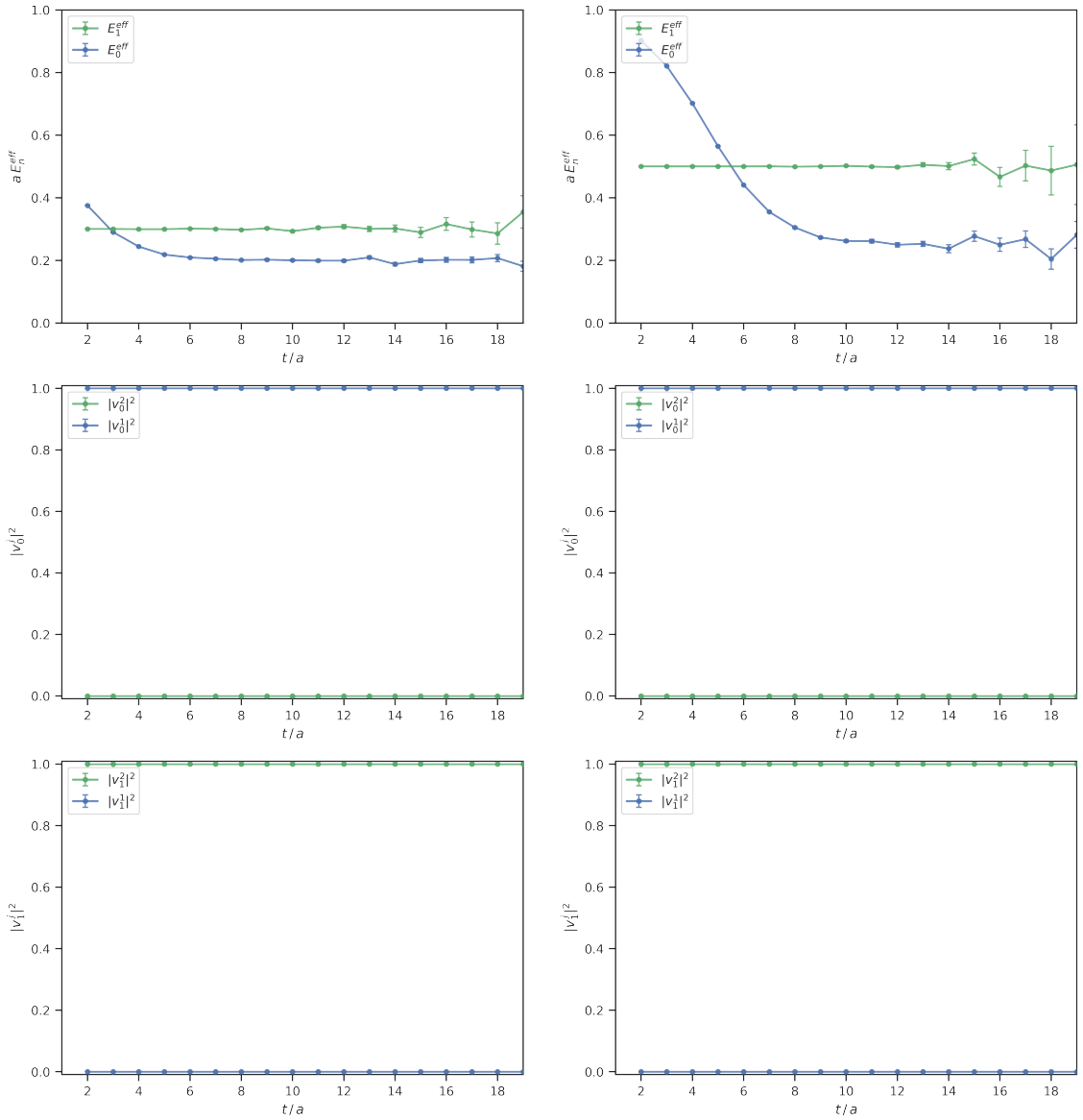

Figure 4.2: Newly sorted effective energies $a\,E_n^{\text{eff}}(t)$ and normalised eigenvector components $|v_n^j(t)|^2$ of the artificial systems 3.2.

Since real data mostly involve correlation matrices with dimensions $d > 2$, larger artificial correlation matrices $C(t)$ are investigated hereafter in preparation for real data sets. For this, Eq. (3.1) is first extended as follows:

$$C(t) = \sum_n \begin{pmatrix} (\psi_n^1)^2 & \psi_n^1\,\psi_n^2 & \psi_n^1\,\psi_n^3 \\ \psi_n^2\,\psi_n^1 & (\psi_n^2)^2 & \psi_n^2\,\psi_n^3 \\ \psi_n^3\,\psi_n^1 & \psi_n^3\,\psi_n^2 & (\psi_n^3)^2 \end{pmatrix} \mathrm{e}^{-E_n\,t} \tag{4.1}$$

and then used to generate artificial data, as described in section 3.2. Therefore, we construct the operator $\mathcal{O}^1$ with both an overlap to the first state E_0 and the fourth state E_3 and the operators $\mathcal{O}^2$ and $\mathcal{O}^3$ with overlaps to the second state

E_1 and the third state E_2. Figure 4.3 shows the effective energies $E_n^{\text{eff}}(t)$ and the eigenvector components $|v_n^j(t)|^2$ of such a system before and after sorting, where $t^{\text{ref}} = 8$ was chosen. As can be seen, the code extension works reliably even with larger correlation matrices and corrects both the erroneous assignment at $t = 8$ and the one at $t = 14$. This illustrates that the application to larger correlation matrices and thus real data is generally possible.

n	ψ_n^1	ψ_n^2	ψ_n^3	E_n
0	0.7	0	0	0.4
1	0	0.5	0.5	0.45
2	0	0.5	-0.5	0.5
3	0.9	0	0	1.0

Table 4.1: Input parameters of the artificial data shown in Figure 4.3.

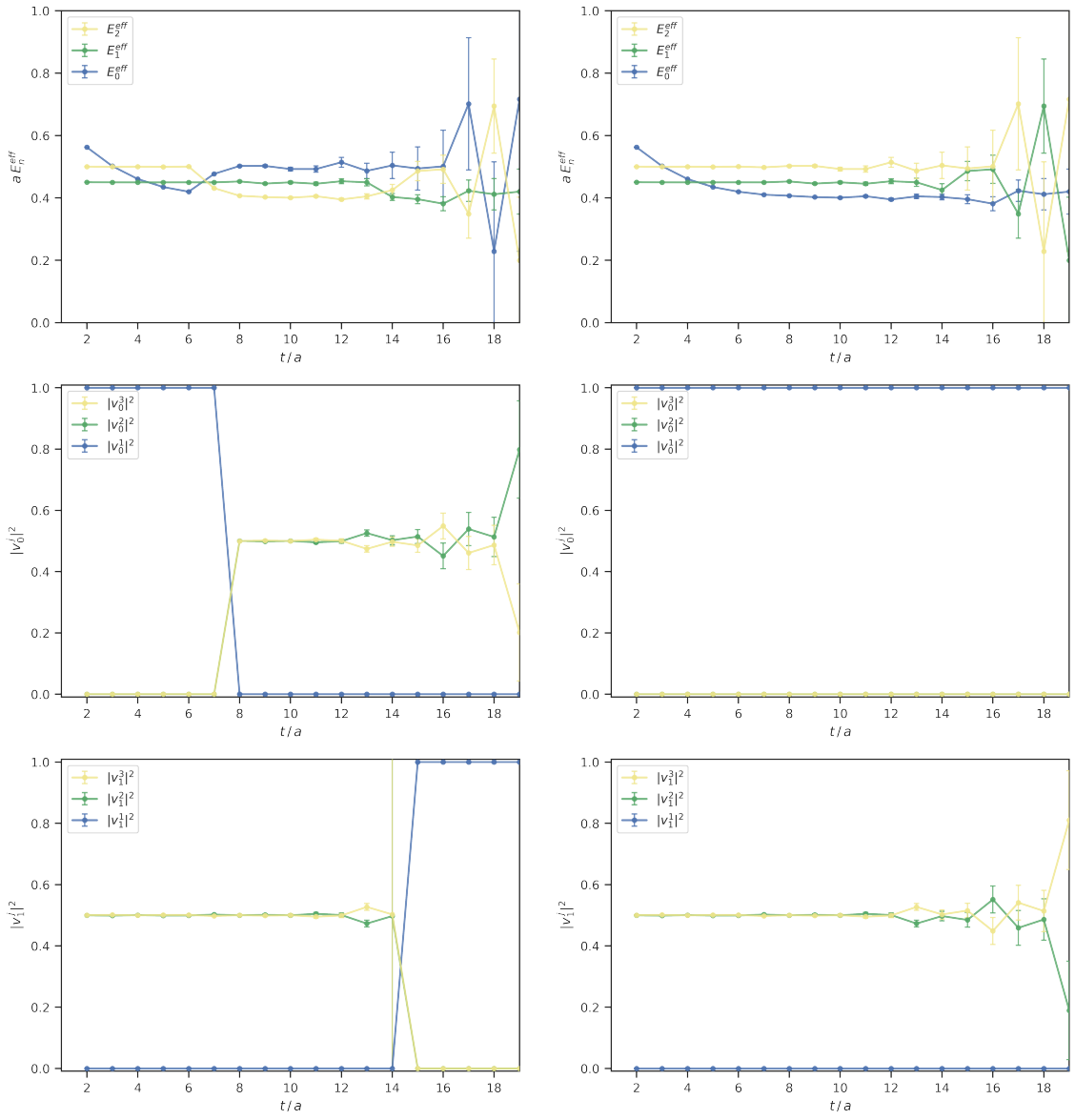

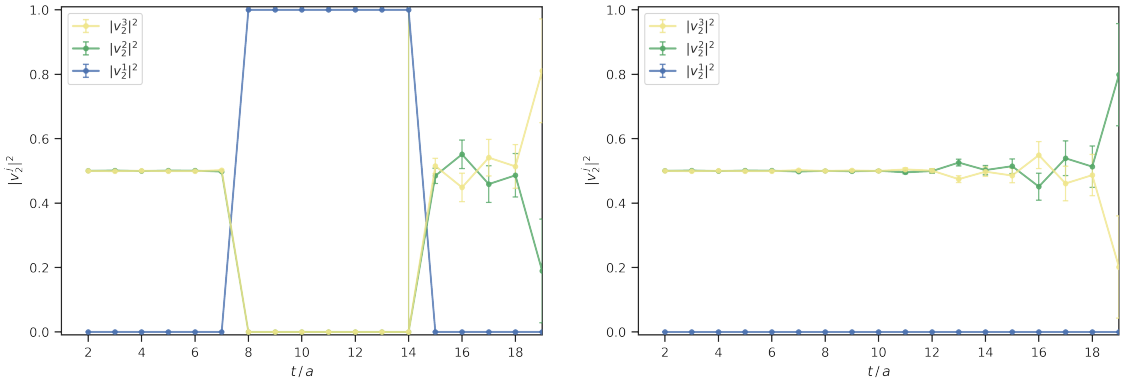

Figure 4.3: Effective energies $a\,E_n^{\text{eff}}(t)$ and eigenvector components $|v_n^j(t)|^2$ of a bigger artificial system before (left) and after (right) the sorting.

4.2 Real Data

During this thesis, only artificially created data have been used so far, both to find possible unintentional behaviour of the program and for subsequent analysis with the newly implemented sorting function. The data extraction from real systems was completely left out. Since the generation of these would go beyond the scope of this thesis, real data from already existing correlation matrices are used in the following section to test and apply the code extension on it [13].

Figure 4.4 shows the effective energies $E_n^{\text{eff}}(t)$ and the normalised eigenvector components $|v_n^j(t)|^2$ of a $\bar{b}\bar{b}us$ tetraquark system before and after the new sorting method, where $t^{\text{ref}} = 8$ was used. It can be observed that the effective energies $E_1^{\text{eff}}(t)$ and $E_2^{\text{eff}}(t)$ hold their plateau slightly longer after sorting. While they were previously stable until $t = 16$ and then disappeard, they now remain stable at their level for about two time units longer. The eigenvector $v_3(t)$ is also more stable after sorting and remains at its original component ratio for $t > 17$. Otherwise, no real improvement can be seen.

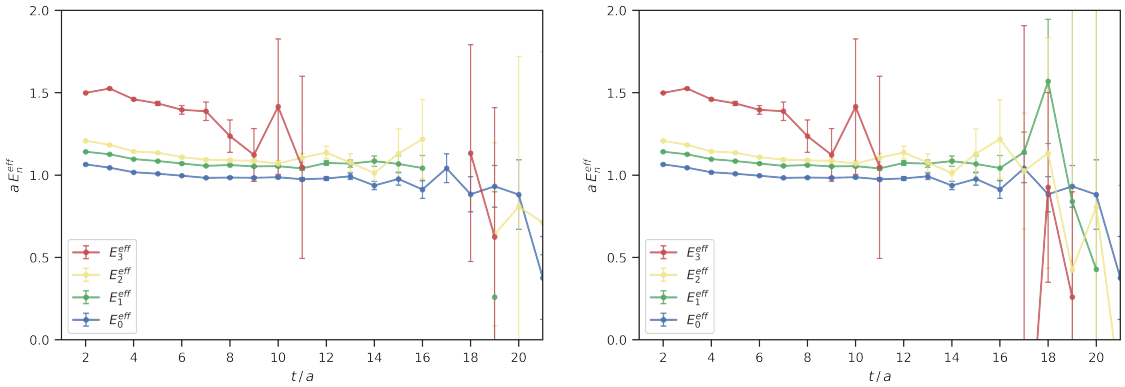

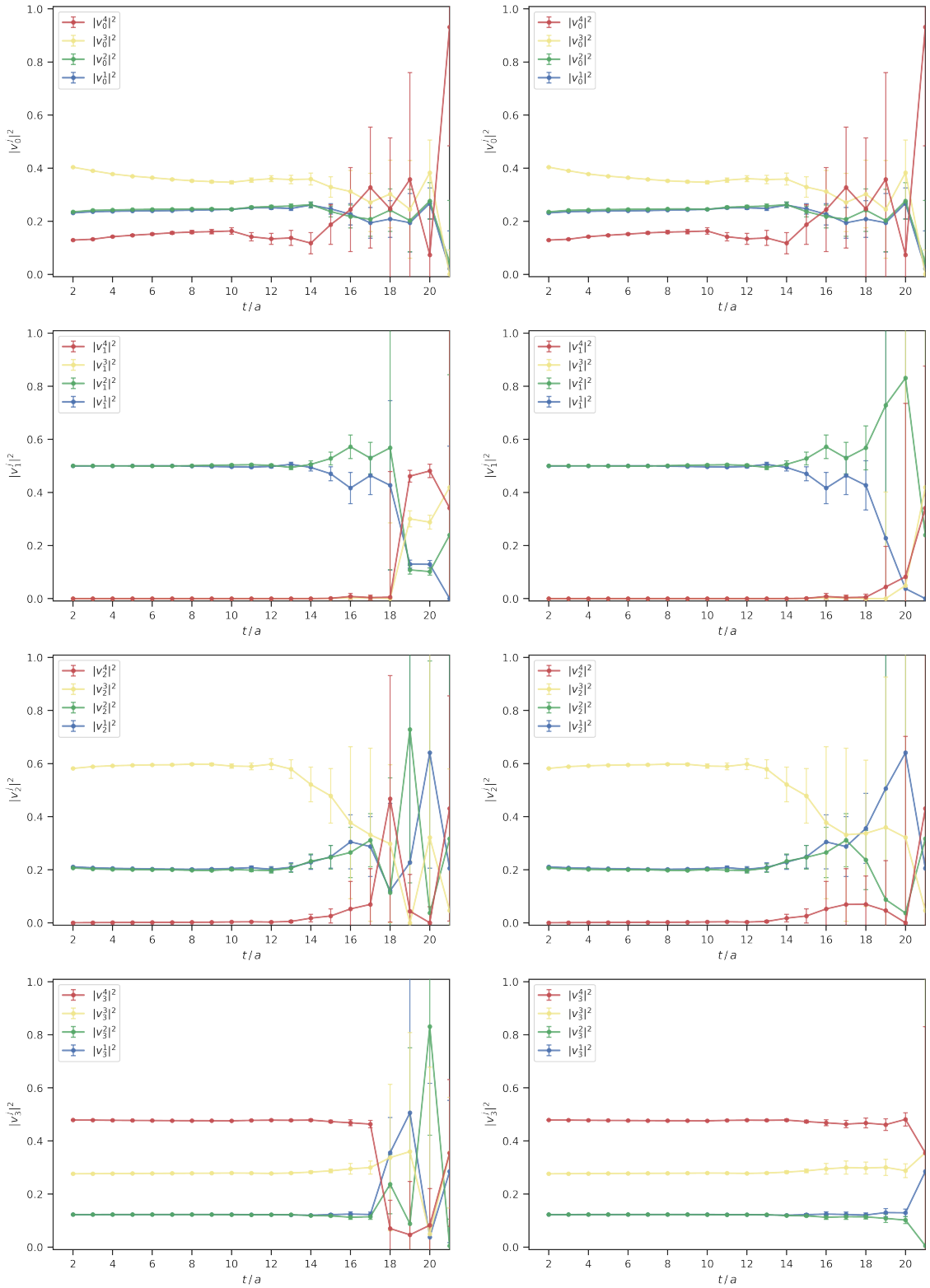

Figure 4.4: Effective energies $a\,E_n^{\text{eff}}(t)$ and eigenvector components $|v_n^j(t)|^2$ of a real $\bar{b}\bar{b}us$ tetraquark system before (left) and after (right) the sorting.

In addition to the above-mentioned $\bar{b}\bar{b}us$ system, other tetraquark systems have been analysed with the new code extension, although no improved results have been achieved so far. Also the system shown in figure 4.4 was already well evaluable

prior to the new sorting. The implementation has therefore not led to any improved analysis, but it has been demonstrated that the sorting works.

Chapter 5

Conclusions and Outlook

The main focus of this thesis was to implement an enhancement of a program for determining hadron masses, which has always produced reliable results. Using artificially produced data, it was possible to locate unexpected behaviour in the sorting of the effective energies $E_n^{\text{eff}}(t)$ that occurred in a small number of systems and to correct it using a newly implemented sorting method. In the case of the examined artificial data, all erroneous behaviour could thus be rectified. With the analysed real data, however, no significant improvement could be observed yet.

Based on the rather insufficient results of the evaluation of the real data, the next step will be to apply the sorting extension to many more different real systems. The focus here will be to investigate the practical usefulness of the code extension. Since the investigated $\bar{b}\bar{b}us$ systems sometimes had 7×7 large correlation matrices, the extension might have reached its limitations there.

Should this also not lead to any improved analyses and results, the next step would be to revise the implemented sorting function and possibly even find a new criterion for sorting.

Appendix A

Bibliography

[1] Cern contributors. "The Standard Model." (2022), [Online]. Available: https://home.cern/science/physics/standard-model.

[2] J. Weber, S. Diehl, T. Kuske and M. Wagner, "An introduction to lattice hadron spectroscopy for students without quantum field theoretical background," 2013. arXiv: 1310.1760.

[3] C. Gattringer and C. B. Lang, *Quantum Chromodynamics on the Lattice*. Springer Science & Business Media, 2009, vol. 788, ISBN: 978-3-642-01849-7.

[4] T. A. DeGrand and C. E. DeTar, *Lattice methods for quantum chromodynamics*. World Scientific, 2006, ISBN: 978-981-256-727-7.

[5] C. Alexandrou, J. Berlin, J. Finkenrath, T. Leontiou and M. Wagner, "Tetraquark interpolating fields in a lattice QCD investigation of the $D^*_{s0}(2317)$ meson," *Physical Review D*, vol. 101, no. 3, 2020. arXiv: 1911.08435.

[6] C. Alexandrou, J. Berlin, M. Dalla Brida, J. Finkenrath, T. Leontiou and M. Wagner, "Lattice QCD investigation of the structure of the $a_0(980)$ meson," *Physical Review D*, vol. 97, no. 3, 2018. arXiv: 1711.09815v2.

[7] C. Hoelbling, "Lattice QCD: concepts, techniques and some results," *Acta Physica Polonica B*, vol. 45, no. 12, 2014. arXiv: 1410.3403.

[8] M. Lüscher and U. Wolff, "How to calculate the elastic scattering matrix in two-dimensional quantum field theories by numerical simulation," *Nuclear Physics B*, vol. 339, no. 1, pp. 222–252, 1990. [Online]. Available: https://www.sciencedirect.com/science/article/pii/055032139090540T.

[9] B. Blossier, M. Della Morte, G. von Hippel, T. Mendes and R. Sommer, "On the generalized eigenvalue method for energies and matrix elements in lattice field theory," *Journal of High Energy Physics*, vol. 2009, no. 04, p. 094, arXiv: 0902.1265.

[10] B. Blossier, G. von Hippel, T. Mendes, R. Sommer and M. Della Morte, "Efficient use of the Generalized Eigenvalue Problem," 2008. arXiv: 0808.1017.

[11] M. Galassi, J. Davies, J. Theiler, B. Gough, G. Jungman, P. Alken, M. Booth and F. Rossi, *GNU Scientific Library Reference Manual*, version 2.7, 2021. [Online]. Available: https://www.gnu.org/software/gsl/doc/html/.

[12] A. McIntosh, "The jackknife estimation method," 2016. arXiv: 1606.00497.

[13] S. Meinel, M. Pflaumer and M. Wagner, "Search for $\bar{b}\bar{b}us$ and $\bar{b}\bar{c}ud$ tetraquark bound states using lattice QCD," *Physical Review D*, vol. 106, 2022. DOI: 10.1103/PhysRevD.106.034507. arXiv: 2205.13982.